

6 Geopotential

Gravitational models commonly used in current (2010) precision orbital analysis represent a significant improvement with respect to geopotential model EGM96, the past conventional model of the IERS Conventions (2003), thanks to the availability of CHAMP ^{<1>} and, most importantly, GRACE ^{<2>} data in the 2000s. The IERS, recognizing the recent development of new gravitational models derived from the optimal combination of GRACE data with high resolution gravitational information obtained from surface gravimetry and satellite altimetry data, recommends at this time the EGM2008 model as the conventional model.

The conventional model that is presented in Section 6.1 describes the static part of the field and the underlying background model for the secular variations of some of its coefficients. In addition, other time varying effects should be taken into account: solid Earth tides (Section 6.2), ocean tides (Section 6.3), solid Earth pole tide (Section 6.4), and ocean pole tide (Section 6.5).

The geopotential field V at the point (r, ϕ, λ) is expanded in spherical harmonics up to degree N as

$$V(r, \phi, \lambda) = \frac{GM}{r} \sum_{n=0}^N \left(\frac{a_e}{r}\right)^n \sum_{m=0}^n [\bar{C}_{nm} \cos(m\lambda) + \bar{S}_{nm} \sin(m\lambda)] \bar{P}_{nm}(\sin \phi) \quad (6.1)$$

(with $\bar{S}_{n0} = 0$), where \bar{C}_{nm} and \bar{S}_{nm} are the normalized geopotential coefficients and \bar{P}_{nm} are the normalized associated Legendre functions. The normalized Legendre function is related to the classical (unnormalized) one by

$$\bar{P}_{nm} = N_{nm} P_{nm}, \quad (6.2a)$$

where

$$N_{nm} = \sqrt{\frac{(n-m)!(2n+1)(2-\delta_{0m})}{(n+m)!}}, \quad \delta_{0m} = \begin{cases} 1 & \text{if } m = 0 \\ 0 & \text{if } m \neq 0 \end{cases} \quad (6.2b)$$

Correspondingly, the normalized geopotential coefficients $(\bar{C}_{nm}, \bar{S}_{nm})$ are related to the unnormalized coefficients (C_{nm}, S_{nm}) by

$$C_{nm} = N_{nm} \bar{C}_{nm}, \quad S_{nm} = N_{nm} \bar{S}_{nm}. \quad (6.3)$$

The scaling parameters (GM, a_e) associated with the model are described in Section 6.1. Sections 6.2 to 6.5 provide variations to the normalized coefficients $(\bar{C}_{nm}, \bar{S}_{nm})$ due to the physical effects described in each section.

6.1 Conventional model based on the EGM2008 model

The EGM2008 model (Pavlis *et al.*, 2008) is complete to degree and order 2159, and contains additional spherical harmonic coefficients up to degree 2190 and order 2159. The GM_{\oplus} and a_e values reported with EGM2008 (398600.4415 km³/s² and 6378136.3 m) should be used as scaling parameters with its gravitational potential coefficients. They are to be considered as TT-compatible values. The recommended TCG-compatible value, $GM_{\oplus} = 398600.4418$ km³/s², should be used with the two-body term when working with Geocentric Coordinate Time (TCG) (398600.4415 or 398600.4356 should be used by those still working with Terrestrial Time (TT) or Barycentric Dynamical Time (TDB), respectively). The EGM2008 model (including error estimates) is available at ^{<3>}.

Although EGM2008 is complete to degree and order 2159, most users in space geodesy will find their needs covered by a truncated version of the model. Suggested truncation levels as a function of the orbit of interest are listed in Table 6.1. It is expected that these truncation levels provide a 3-dimensional orbit accuracy of better than 0.5 mm for the indicated satellites (Ries, 2010).

¹<http://op.gfz-potsdam.de/champ/>

²<http://www.csr.utexas.edu/grace/>

³<http://earth-info.nga.mil/GandG/wgs84/gravitymod/egm2008/>

Table 6.1: Suggested truncation levels for use of EGM2008 at different orbits

Orbit radius / km	Example	Truncation level
7331	Starlette	90
12270	Lageos	20
26600	GPS	12

The EGM2008 model was based on the ITG-GRACE03S GRACE-only gravitational model ($\langle^4\rangle$, see also Mayer-Gürr, 2007) which is available along with its complete error covariance matrix to degree and order 180. Therefore the static gravitational field was developed assuming models complying with the IERS Conventions (2003) and complemented by the following:

- ocean tides: FES2004 (Lyard *et al.*, 2006),
- ocean pole tide: Desai (2003, see Section 6.5),
- atmosphere and ocean de-aliasing: AOD1B RL04 (Flechtner, 2007).

For some of the low-degree coefficients, the conventional geopotential model uses values which are different from the original EGM2008 values. The static field also assumes values for the secular rates of low-degree coefficients. In order to use the static field properly and project it in time, the secular rates should be accounted for. The instantaneous values of coefficients \bar{C}_{n0} to be used when computing orbits are given by:

$$\bar{C}_{n0}(t) = \bar{C}_{n0}(t_0) + d\bar{C}_{n0}/dt \times (t - t_0) \quad (6.4)$$

where t_0 is the epoch J2000.0 and the values of $\bar{C}_{n0}(t_0)$ and $d\bar{C}_{n0}/dt$ are given in Table 6.2. Note that the zero-tide C_{20} coefficient in the conventional geopotential model is obtained from the analysis of 17 years of SLR data approximately centered on year 2000 and has an uncertainty of 2×10^{-11} (Cheng *et al.*, 2010). It differs significantly from the EGM2008 value obtained from 4 years of GRACE data, as it is expected that tide-like aliases will affect GRACE-based C_{20} values, depending on the averaging interval used. The tide-free value of C_{20} can be obtained as described in Section 6.2.2.

Table 6.2: Low-degree coefficients of the conventional geopotential model

Coefficient	Value at 2000.0	Reference	Rate / yr ⁻¹	Reference
\bar{C}_{20} (zero-tide)	$-0.48416948 \times 10^{-3}$	Cheng <i>et al.</i> , 2010	11.6×10^{-12}	Nerem <i>et al.</i> , 1993
\bar{C}_{30}	0.9571612×10^{-6}	EGM2008	4.9×10^{-12}	Cheng <i>et al.</i> , 1997
\bar{C}_{40}	0.5399659×10^{-6}	EGM2008	4.7×10^{-12}	Cheng <i>et al.</i> , 1997

Values for the C_{21} and S_{21} coefficients are included in the conventional geopotential model. The C_{21} and S_{21} coefficients describe the position of the Earth's figure axis. When averaged over many years, the figure axis should closely coincide with the observed position of the rotation pole averaged over the same time period. Any differences between the averaged positions of the mean figure and the mean rotation pole would be due to long-period fluid motions in the atmosphere, oceans, or Earth's fluid core (Wahr, 1987; 1990). At present, there is no independent evidence that such motions are important. The conventional values for $C_{21}(t)$ and $S_{21}(t)$ are intended to give a mean figure axis that corresponds to the mean pole position consistent with the terrestrial reference frame defined in Chapter 4.

This choice for C_{21} and S_{21} is realized as follows. First, to use the gravitational potential coefficients to solve for a satellite orbit, it is necessary to rotate from

⁴<http://www.igg.uni-bonn.de/apmg/fileadmin/itg-grace03.html>

the Earth-fixed frame, where the coefficients are pertinent, to an inertial frame, where the satellite motion is computed. This transformation between frames should include polar motion. We assume the polar motion parameters used are relative to the IERS Reference Pole. Then the values

$$\begin{aligned}\bar{C}_{21}(t) &= \sqrt{3}\bar{x}_p(t)\bar{C}_{20} - \bar{x}_p(t)\bar{C}_{22} + \bar{y}_p(t)\bar{S}_{22}, \\ \bar{S}_{21}(t) &= -\sqrt{3}\bar{y}_p(t)\bar{C}_{20} - \bar{y}_p(t)\bar{C}_{22} - \bar{x}_p(t)\bar{S}_{22},\end{aligned}\quad (6.5)$$

where $\bar{x}_p(t)$ and $\bar{y}_p(t)$ (in radians) represent the IERS conventional mean pole (see Section 7.1.4), provide a mean figure axis which coincides with the mean pole consistent with the TRF defined in Chapter 4. Any recent value of \bar{C}_{20} , \bar{C}_{22} and \bar{S}_{22} is adequate for 10^{-14} accuracy in Equation (6.5), e.g. the values of the present conventional model ($-0.48416948 \times 10^{-3}$, 2.4393836×10^{-6} and $-1.4002737 \times 10^{-6}$ respectively) can be used.

The models for the low degree terms are generally consistent with the past long-term trends, but these are not strictly linear in reality. There may be decadal variations that are not captured by the models. In addition, they may not be consistent with more recent surface mass trends due to increased ice sheet melting and other results of global climate change.

6.2 Effect of solid Earth tides

6.2.1 Conventional model for the solid Earth tides

The changes induced by the solid Earth tides in the free space potential are most conveniently modeled as variations in the standard geopotential coefficients C_{nm} and S_{nm} (Eanes *et al.*, 1983). The contributions ΔC_{nm} and ΔS_{nm} from the tides are expressible in terms of the Love number k . The effects of ellipticity and of the Coriolis force due to Earth rotation on tidal deformations necessitate the use of three k parameters, $k_{nm}^{(0)}$ and $k_{nm}^{(\pm)}$ (except for $n = 2$) to characterize the changes produced in the free space potential by tides of spherical harmonic degree and order (nm) (Wahr, 1981); only two parameters are needed for $n = 2$ because $k_{2m}^{(-)} = 0$ due to mass conservation.

Anelasticity of the mantle causes $k_{nm}^{(0)}$ and $k_{nm}^{(\pm)}$ to acquire small imaginary parts (reflecting a phase lag in the deformational response of the Earth to tidal forces), and also gives rise to a variation with frequency which is particularly pronounced within the long period band. Though modeling of anelasticity at the periods relevant to tidal phenomena (8 hours to 18.6 years) is not yet definitive, it is clear that the magnitudes of the contributions from anelasticity cannot be ignored (see below). Recent evidence relating to the role of anelasticity in the accurate modeling of nutation data (Mathews *et al.*, 2002) lends support to the model employed herein, at least up to diurnal tidal periods; and there is no compelling reason at present to adopt a different model for the long period tides.

Solid Earth tides within the diurnal tidal band (for which $(nm) = (21)$) are not wholly due to the direct action of the tide generating potential (TGP) on the solid Earth; they include the deformations (and associated geopotential changes) arising from other effects of the TGP, namely, ocean tides and wobbles of the mantle and the core regions. Deformation due to wobbles arises from the incremental centrifugal potentials caused by the wobbles; and ocean tides load the crust and thus cause deformations. Anelasticity affects the Earth's deformational response to all these types of forcing.

The wobbles, in turn, are affected by changes in the Earth's moment of inertia due to deformations from all sources, and in particular, from the deformation due to loading by the $(nm) = (21)$ part of the ocean tide; wobbles are also affected by the anelasticity contributions to all deformations, and by the coupling of the fluid core to the mantle and the inner core through the action of magnetic fields at its boundaries (Mathews *et al.*, 2002). Resonances in the wobbles—principally, the Nearly Diurnal Free Wobble resonance associated with the FCN—and the consequent resonances in the contribution to tidal deformation from the centrifugal perturbations associated with the wobbles, cause the body tide and load Love/Shida

number parameters of the diurnal tides to become strongly frequency dependent. For the derivation of resonance formulae of the form (6.9) below to represent this frequency dependence, see Mathews *et al.*, (1995). The resonance expansions assume that the Earth parameters entering the wobble equations are all frequency independent. However the ocean tide induced deformation makes a frequency dependent contribution to deformability parameters which are among the Earth parameters just referred to. It becomes necessary therefore to add small corrections to the Love number parameters computed using the resonance formulae. These corrections are included in the tables of Love number parameters given in this chapter and the next.

The deformation due to ocean loading is itself computed in the first place using frequency independent load Love numbers (see Section 7.1.2). Corrections to take account of the resonances in the load Love numbers are incorporated through equivalent corrections to the *body tide* Love numbers, following Wahr and Sasao (1981), as explained further below. These corrections are also included in the tables of Love numbers.

The degree 2 tides produce time dependent changes in C_{2m} and S_{2m} , through $k_{2m}^{(0)}$, which can exceed 10^{-8} in magnitude. They also produce changes exceeding 3×10^{-12} in C_{4m} and S_{4m} through $k_{2m}^{(+)}$. (The direct contributions of the degree 4 tidal potential to these coefficients are negligible.) The only other changes exceeding this cutoff are in C_{3m} and S_{3m} , produced by the degree 3 part of the TGP.

The computation of the tidal contributions to the geopotential coefficients is most efficiently done by a three-step procedure. In Step 1, the $(2m)$ part of the tidal potential is evaluated in the time domain for each m using lunar and solar ephemerides, and the corresponding changes ΔC_{2m} and ΔS_{2m} are computed using frequency independent nominal values k_{2m} for the respective $k_{2m}^{(0)}$. The contributions of the degree 3 tides to C_{3m} and S_{3m} through $k_{3m}^{(0)}$ and also those of the degree 2 tides to C_{4m} and S_{4m} through $k_{2m}^{(+)}$ may be computed by a similar procedure; they are at the level of 10^{-11} .

Step 2 corrects for the deviations of the $k_{21}^{(0)}$ of several of the constituent tides of the diurnal band from the constant nominal value k_{21} assumed for this band in the first step. Similar corrections need to be applied to a few of the constituents of the other two bands also.

Steps 1 and 2 can be used to compute the total tidal contribution, including the time independent (permanent) contribution to the geopotential coefficient \bar{C}_{20} , which is adequate for a “conventional tide free” model such as EGM96. When using a “zero tide” model, this permanent part should not be counted twice, this is the goal of Step 3 of the computation. See Section 6.2.2.

With frequency-independent values k_{nm} (Step 1), changes induced by the (nm) part of the TGP in the normalized geopotential coefficients having the same (nm) are given in the time domain by

$$\Delta \bar{C}_{nm} - i \Delta \bar{S}_{nm} = \frac{k_{nm}}{2n+1} \sum_{j=2}^3 \frac{GM_j}{GM_{\oplus}} \left(\frac{R_e}{r_j} \right)^{n+1} \bar{P}_{nm}(\sin \Phi_j) e^{-im\lambda_j} \quad (6.6)$$

where

k_{nm} = nominal Love number for degree n and order m ,

R_e = equatorial radius of the Earth,

GM_{\oplus} = gravitational parameter for the Earth,

GM_j = gravitational parameter for the Moon ($j = 2$) and Sun ($j = 3$),

r_j = distance from geocenter to Moon or Sun,

Φ_j = body-fixed geocentric latitude of Moon or Sun,

λ_j = body-fixed east longitude (from Greenwich) of Moon or Sun.

Equation (6.6) yields $\Delta\bar{C}_{nm}$ and $\Delta\bar{S}_{nm}$ for both $n = 2$ and $n = 3$ for all m , apart from the corrections for frequency dependence to be evaluated in Step 2. (The particular case $(nm) = (20)$ needs special consideration, however, as already indicated.)

One further computation to be done in Step 1 is that of the changes in the degree 4 coefficients produced by the degree 2 tides. They are given by

$$\Delta\bar{C}_{4m} - i\Delta\bar{S}_{4m} = \frac{k_{2m}^{(+)}}{5} \sum_{j=2}^3 \frac{GM_j}{GM_{\oplus}} \left(\frac{R_e}{r_j}\right)^3 \bar{P}_{2m}(\sin \Phi_j) e^{-im\lambda_j}, \quad (m = 0, 1, 2), \quad (6.7)$$

which has the same form as Equation (6.6) for $n = 2$ except for the replacement of k_{2m} by $k_{2m}^{(+)}$.

The parameter values for the computations of Step 1 are given in Table 6.3. The choice of these nominal values has been made so as to minimize the number of terms for which corrections will have to be applied in Step 2. The nominal value for $m = 0$ has to be chosen real because there is no closed expression for the contribution to \bar{C}_{20} from the imaginary part of $k_{20}^{(0)}$.

Table 6.3: Nominal values of solid Earth tide external potential Love numbers.

		Elastic Earth		Anelastic Earth		
n	m	k_{nm}	$k_{nm}^{(+)}$	Re k_{nm}	Im k_{nm}	$k_{nm}^{(+)}$
2	0	0.29525	-0.00087	0.30190	-0.00000	-0.00089
2	1	0.29470	-0.00079	0.29830	-0.00144	-0.00080
2	2	0.29801	-0.00057	0.30102	-0.00130	-0.00057
3	0	0.093	...			
3	1	0.093	...			
3	2	0.093	...			
3	3	0.094	...			

The frequency dependent corrections to the $\Delta\bar{C}_{nm}$ and $\Delta\bar{S}_{nm}$ values obtained from Step 1 are computed in Step 2 as the sum of contributions from a number of tidal constituents belonging to the respective bands. The contribution to $\Delta\bar{C}_{20}$ from the long period tidal constituents of various frequencies f is

$$\text{Re} \sum_{f(2,0)} (A_0 \delta k_f H_f) e^{i\theta_f} = \sum_{f(2,0)} [(A_0 H_f \delta k_f^R) \cos \theta_f - (A_0 H_f \delta k_f^I) \sin \theta_f], \quad (6.8a)$$

while the contribution to $(\Delta\bar{C}_{21} - i\Delta\bar{S}_{21})$ from the diurnal tidal constituents and to $\Delta\bar{C}_{22} - i\Delta\bar{S}_{22}$ from the semidiurnals are given by

$$\Delta\bar{C}_{2m} - i\Delta\bar{S}_{2m} = \eta_m \sum_{f(2,m)} (A_m \delta k_f H_f) e^{i\theta_f}, \quad (m = 1, 2), \quad (6.8b)$$

where

$$A_0 = \frac{1}{R_e \sqrt{4\pi}} = 4.4228 \times 10^{-8} \text{ m}^{-1}, \quad (6.8c)$$

$$A_m = \frac{(-1)^m}{R_e \sqrt{8\pi}} = (-1)^m (3.1274 \times 10^{-8}) \text{ m}^{-1}, \quad (m \neq 0), \quad (6.8d)$$

$$\eta_1 = -i, \quad \eta_2 = 1, \quad (6.8e)$$

δk_f = difference between k_f defined as $k_{2m}^{(0)}$ at frequency f and the nominal value k_{2m} , in the sense $k_f - k_{2m}$, plus a contribution from ocean loading,

δk_f^R = real part of δk_f , and

δk_f^I = imaginary part of δk_f , i.e., $\delta k_f = \delta k_f^R + i\delta k_f^I$,

H_f = amplitude (in meters) of the term at frequency f from the harmonic expansion of the tide generating potential, defined according to the convention of Cartwright and Tayler (1971), and

$$\begin{aligned}\theta_f &= \bar{n} \cdot \bar{\beta} = \sum_{i=1}^6 n_i \beta_i, \quad \text{or} \\ \theta_f &= m(\theta_g + \pi) - \bar{N} \cdot \bar{F} = m(\theta_g + \pi) - \sum_{j=1}^5 N_j F_j,\end{aligned}$$

where

$\bar{\beta}$ = six-vector of Doodson's fundamental arguments β_i ,
(τ, s, h, p, N', p_s),

\bar{n} = six-vector of multipliers n_i (for the term at frequency f) of the fundamental arguments,

\bar{F} = five-vector of fundamental arguments F_j
(the Delaunay variables l, l', F, D, Ω) of nutation theory,

\bar{N} = five-vector of multipliers N_j of the Delaunay variables for the nutation of frequency $-f + d\theta_g/dt$,

and θ_g is the Greenwich Mean Sidereal Time expressed in angle units (i.e. 24 h = 360°; see Chapter 5).

(π in $(\theta_g + \pi)$ is now to be replaced by 180°.)

For the fundamental arguments (l, l', F, D, Ω) of nutation theory and the convention followed here in choosing their multipliers N_j , see Chapter 5. For conversion of tidal amplitudes defined according to different conventions to the amplitude H_f corresponding to the Cartwright-Tayler convention, use Table 6.8 given at the end of this chapter.

For diurnal tides, the frequency dependent values of any load or body tide Love number parameter L (such as $k_{21}^{(0)}$ or $k_{21}^{(+)}$ in the present context) may be represented as a function of the tidal excitation frequency σ by a resonance formula

$$L(\sigma) = L_0 + \sum_{\alpha=1}^3 \frac{L_\alpha}{(\sigma - \sigma_\alpha)}, \quad (6.9)$$

except for the small corrections referred to earlier. (They are to take account of frequency dependent contributions to a few of the Earth's deformability parameters, which make (6.9) inexact.) The σ_α , ($\alpha = 1, 2, 3$), are the respective resonance frequencies associated with the Chandler wobble (CW), the retrograde FCN, and the prograde free core nutation (also known as the free inner core nutation), and the L_α are the corresponding resonance coefficients. All the parameters are complex. The σ_α and σ are expressed in cycles per sidereal day (cpsd), with the convention that positive (negative) frequencies represent retrograde (prograde) waves. (This sign convention, followed in tidal theory, is the opposite of that employed in analytical theories of nutation.) In particular, given the tidal frequency f in degrees per hour, one has

$$\sigma = f/(15 \times 1.002737909),$$

the factor 1.002737909 being the number of sidereal days per solar day. The values used herein for the σ_α are from Mathews *et al.* (2002), adapted to the sign

convention used here:

$$\begin{aligned}\sigma_1 &= -0.0026010 - 0.0001361 i \\ \sigma_2 &= 1.0023181 + 0.000025 i \\ \sigma_3 &= 0.999026 + 0.000780 i.\end{aligned}\tag{6.10}$$

They were estimated from a fit of nutation theory to precession rate and nutation amplitude estimates found from an analysis of very long baseline interferometry (VLBI) data.

Table 6.4 lists the values of L_0 and L_α in resonance formulae of the form (6.9) for $k_{21}^{(0)}$ and $k_{21}^{(+)}$. They were obtained by evaluating the relevant expressions from Mathews *et al.* (1995), using values taken from computations of Buffett and Mathews (unpublished) for the needed deformability parameters together with values obtained for the wobble resonance parameters in the course of computations of the nutation results of Mathews *et al.* (2002). The deformability parameters for an elliptical, rotating, elastic, and oceanless Earth model based on the 1-second reference period preliminary reference Earth model (PREM) (Dziewonski and Anderson, 1981) with the ocean layer replaced by solid, and corrections to these for the effects of mantle anelasticity, were found by integration of the tidal deformation equations. Anelasticity computations were based on the Widmer *et al.* (1991) model of mantle Q . As in Wahr and Bergen (1986), a power law was assumed for the frequency dependence of Q , with 200 s as the reference period; the value $\alpha = 0.15$ was used for the power law index. The anelasticity contribution (out-of-phase and in-phase) to the tidal changes in the geopotential coefficients is at the level of 1 – 2% in-phase, and 0.5 – 1% out-of-phase, *i.e.*, of the order of 10^{-10} . The effects of anelasticity, ocean loading and currents, and electromagnetic couplings on the wobbles result in indirect contributions to $k_{21}^{(0)}$ and $k_{21}^{(+)}$ which are almost fully accounted for through the values of the wobble resonance parameters. Also shown in Table 6.4 are the resonance parameters for the load Love numbers h'_{21} , k'_{21} , and l'_{21} , which are relevant to the solid Earth deformation caused by ocean tidal loading and to the consequential changes in the geopotential. (Only the real parts are shown: the small imaginary parts make no difference to the effect to be now considered which is itself small.)

Table 6.4: Parameters in the resonance formulae for $k_{21}^{(0)}$, $k_{21}^{(+)}$ and the load Love numbers.

α	$k_{21}^{(0)}$		$k_{21}^{(+)}$	
	Re L_α	Im L_α	Re L_α	Im L_α
0	0.29954	-0.1412×10^{-2}	-0.804×10^{-3}	0.237×10^{-5}
1	-0.77896×10^{-3}	-0.3711×10^{-4}	0.209×10^{-5}	0.103×10^{-6}
2	0.90963×10^{-4}	-0.2963×10^{-5}	-0.182×10^{-6}	0.650×10^{-8}
3	-0.11416×10^{-5}	0.5325×10^{-7}	-0.713×10^{-9}	-0.330×10^{-9}
Load Love numbers (Real parts only)				
	h'_{21}	l'_{21}	k'_{21}	
0	-0.99500	0.02315	-0.30808	
1	1.6583×10^{-3}	2.3232×10^{-4}	8.1874×10^{-4}	
2	2.8018×10^{-4}	-8.4659×10^{-6}	1.4116×10^{-4}	
3	5.5852×10^{-7}	1.0724×10^{-8}	3.4618×10^{-7}	

The expressions given in Section 6.3 for the contributions from ocean tidal loading assume the constant nominal value $k_2'^{(\text{nom})} = -0.3075$ for k' of the degree 2 tides. Further contributions arise from the frequency dependence of k'_{21} . These may be expressed, following Wahr and Sasao (1981), in terms of an effective ocean tide contribution $\delta k^{(OT)}(\sigma)$ to the body tide Love number $k_{21}^{(0)}$:

$$\delta k^{(OT)}(\sigma) = [k'_{21}(\sigma) - k_2'^{(\text{nom})}] \left(\frac{4\pi G \rho_w R}{5\bar{g}} \right) A_{21}(\sigma),\tag{6.11}$$

where G is the constant of universal gravitation, ρ_w is the density of sea water (1025 kg m^{-3}), R is the Earth's mean radius ($6.371 \times 10^6 \text{ m}$), \bar{g} is the mean acceleration due to gravity at the Earth's surface (9.820 m s^{-2}), and $A_{21}(\sigma)$ is the admittance for the degree 2 tesseral component of the ocean tide of frequency σ in cpsd:

$$A_{21}(\sigma) = \zeta_{21}(\sigma)/\bar{H}(\sigma).$$

ζ_{21} is the complex amplitude of the height of the $(nm) = (21)$ component of the ocean tide, and \bar{H} is the height equivalent of the amplitude of the tide generating potential, the bar being a reminder that the spherical harmonics used in defining the two amplitudes should be identically normalized. Wahr and Sasao (1981) employed the factorized form

$$A_{21}(\sigma) = f_{FCN}(\sigma) f_{OD}(\sigma),$$

wherein the first factor represents the effect of the FCN resonance, and the second, that of other ocean dynamic factors. The following empirical formulae (Mathews *et al.*, 2002) which provide good fits to the FCN factors of a set of 11 diurnal tides (Desai and Wahr, 1995) and to the admittances obtainable from the ocean load angular momenta of four principal tides (Chao *et al.*, 1996) are used herein:

$$\begin{aligned} f_{OD}(\sigma) &= (1.3101 - 0.8098 i) - (1.1212 - 0.6030 i)\sigma, \\ f_{FCN}(\sigma) &= 0.1732 + 0.9687 f_{eqm}(\sigma), \\ f_{eqm}(\sigma) &= \frac{\gamma(\sigma)}{1 - (3\rho_w/5\bar{\rho})\gamma'(\sigma)}, \end{aligned}$$

where $\gamma = 1 + k - h$ and $\gamma' = 1 + k' - h'$, $\bar{\rho}$ is the Earth's mean density. (Here k stands for $k_{21}^{(0)}$, and similarly for the other symbols. Only the real parts need be used.) f_{eqm} is the FCN factor for a global equilibrium ocean.

Table 6.5a shows the values of

$$\delta k_f \equiv (k_{21}^{(0)}(\sigma) - k_{21}) + \delta k_{21}^{OT}(\sigma),$$

along with the real and imaginary parts of the amplitude ($A_1 \delta k_f H_f$). The tides listed are those for which either of the parts is at least 10^{-13} after round-off. (A cutoff at this level is used for the individual terms in order that accuracy at the level of 3×10^{-12} be not affected by the accumulated contributions from the numerous smaller terms that are disregarded.) Roughly half the value of the imaginary part comes from the ocean tide term, and the real part contribution from this term is of about the same magnitude.

The values used for $k_{21}^{(0)}(\sigma)$ in evaluating δk_f are from an exact computation necessarily involving use of the framework of nutation-wobble theory which is outside the scope of this chapter. If the (approximate) resonance formula were used instead for the computation, the resulting numbers for δk_f^R and δk_f^I would require small corrections to match the exact values. In units of 10^{-5} , they are (in-phase, out-of-phase) (1, 1) for Q_1 , (1, 1) for O_1 and its companion having Doodson numbers 145,545, (1, 0) for NO_1 , (0, -1) for P_1 , (244, 299) for ψ_1 , (12, 12) for ϕ_1 , (3, 2) for J_1 , and (2, 1) for Oo_1 and its companion with Doodson numbers 185,565. These are the only tides for which the corrections would contribute nonnegligibly to the numbers listed in the last two columns of the table.

Calculation of the correction due to any tidal constituent is illustrated by the following example for K_1 . Given that $A_m = A_1 = -3.1274 \times 10^{-8}$, and that $H_f = 0.36870$, $\theta_f = (\theta_g + \pi)$, and $k_{21}^{(0)} = (0.25746 + 0.00118 i)$ for this tide, one finds on subtracting the nominal value ($0.29830 - 0.00144 i$) that $\delta k_f = (-0.04084 + 0.00262 i)$. Equation (6.8b) then yields:

$$\begin{aligned} (\Delta \bar{C}_{21})_{K_1} &= 470.9 \times 10^{-12} \sin(\theta_g + \pi) - 30.2 \times 10^{-12} \cos(\theta_g + \pi), \\ (\Delta \bar{S}_{21})_{K_1} &= 470.9 \times 10^{-12} \cos(\theta_g + \pi) + 30.2 \times 10^{-12} \sin(\theta_g + \pi). \end{aligned}$$

Table 6.5a: The in-phase (*ip*) amplitudes ($A_1\delta k_f^R H_f$) and the out-of-phase (*op*) amplitudes ($A_1\delta k_f^I H_f$) of the corrections for frequency dependence of $k_{21}^{(0)}$, taking the nominal value k_{21} for the diurnal tides as $(0.29830 - i0.00144)$. Units: 10^{-12} . The entries for δk_f^R and δk_f^I are in units of 10^{-5} . Multipliers of the Doodson arguments identifying the tidal terms are given, as also those of the Delaunay variables characterizing the nutations produced by these terms.

Name	deg/hr	Doodson No.	τ	s	h	p	N'	p_s	ℓ	ℓ'	F	D	Ω	δk_f^R / 10^{-5}	δk_f^I / 10^{-5}	Amp. (<i>ip</i>)	Amp. (<i>op</i>)
2Q ₁	12.85429	125,755	1	-3	0	2	0	0	2	0	2	0	2	-29	3	-0.1	0.0
σ_1	12.92714	127,555	1	-3	2	0	0	0	0	0	2	2	2	-30	3	-0.1	0.0
	13.39645	135,645	1	-2	0	1	-1	0	1	0	2	0	1	-45	5	-0.1	0.0
Q ₁	13.39866	135,655	1	-2	0	1	0	0	1	0	2	0	2	-46	5	-0.7	0.1
ρ_1	13.47151	137,455	1	-2	2	-1	0	0	-1	0	2	2	2	-49	5	-0.1	0.0
	13.94083	145,545	1	-1	0	0	-1	0	0	0	2	0	1	-82	7	-1.3	0.1
O ₁	13.94303	145,555	1	-1	0	0	0	0	0	0	2	0	2	-83	7	-6.8	0.6
τ_1	14.02517	147,555	1	-1	2	0	0	0	0	0	0	2	0	-91	9	0.1	0.0
N τ_1	14.41456	153,655	1	0	-2	1	0	0	1	0	2	-2	2	-168	14	0.1	0.0
	14.48520	155,445	1	0	0	-1	-1	0	-1	0	2	0	1	-193	16	0.1	0.0
Lk ₁	14.48741	155,455	1	0	0	-1	0	0	-1	0	2	0	2	-194	16	0.4	0.0
No ₁	14.49669	155,655	1	0	0	1	0	0	1	0	0	0	0	-197	16	1.3	-0.1
	14.49890	155,665	1	0	0	1	1	0	1	0	0	0	1	-198	16	0.3	0.0
χ_1	14.56955	157,455	1	0	2	-1	0	0	-1	0	0	2	0	-231	18	0.3	0.0
	14.57176	157,465	1	0	2	-1	1	0	-1	0	0	2	1	-233	18	0.1	0.0
π_1	14.91787	162,556	1	1	-3	0	0	1	0	1	2	-2	2	-834	58	-1.9	0.1
	14.95673	163,545	1	1	-2	0	-1	0	0	0	2	-2	1	-1117	76	0.5	0.0
P ₁	14.95893	163,555	1	1	-2	0	0	0	0	0	2	-2	2	-1138	77	-43.4	2.9
	15.00000	164,554	1	1	-1	0	0	-1	0	-1	2	-2	2	-1764	104	0.6	0.0
S ₁	15.00000	164,556	1	1	-1	0	0	1	0	1	0	0	0	-1764	104	1.6	-0.1
	15.02958	165,345	1	1	0	-2	-1	0	-2	0	2	0	1	-3048	92	0.1	0.0
	15.03665	165,535	1	1	0	0	-2	0	0	0	0	0	-2	-3630	195	0.1	0.0
	15.03886	165,545	1	1	0	0	-1	0	0	0	0	0	-1	-3845	229	-8.8	0.5
K ₁	15.04107	165,555	1	1	0	0	0	0	0	0	0	0	0	-4084	262	470.9	-30.2
	15.04328	165,565	1	1	0	0	1	0	0	0	0	0	1	-4355	297	68.1	-4.6
	15.04548	165,575	1	1	0	0	2	0	0	0	0	0	2	-4665	334	-1.6	0.1
	15.07749	166,455	1	1	1	-1	0	0	-1	0	0	1	0	85693	21013	0.1	0.0
	15.07993	166,544	1	1	1	0	-1	-1	0	-1	0	0	-1	35203	2084	-0.1	0.0
ψ_1	15.08214	166,554	1	1	1	0	0	-1	0	-1	0	0	0	22794	358	-20.6	-0.3
	15.08214	166,556	1	1	1	0	0	1	0	1	-2	2	-2	22780	358	0.3	0.0
	15.08434	166,564	1	1	1	0	1	-1	0	-1	0	0	1	16842	-85	-0.3	0.0
	15.11392	167,355	1	1	2	-2	0	0	-2	0	0	2	0	3755	-189	-0.2	0.0
	15.11613	167,365	1	1	2	-2	1	0	-2	0	0	2	1	3552	-182	-0.1	0.0
ϕ_1	15.12321	167,555	1	1	2	0	0	0	0	0	-2	2	-2	3025	-160	-5.0	0.3
	15.12542	167,565	1	1	2	0	1	0	0	0	-2	2	-1	2892	-154	0.2	0.0
	15.16427	168,554	1	1	3	0	0	-1	0	-1	-2	2	-2	1638	-93	-0.2	0.0
θ_1	15.51259	173,655	1	2	-2	1	0	0	1	0	0	-2	0	370	-20	-0.5	0.0
	15.51480	173,665	1	2	-2	1	1	0	1	0	0	-2	1	369	-20	-0.1	0.0
	15.58323	175,445	1	2	0	-1	-1	0	-1	0	0	0	-1	325	-17	0.1	0.0
J ₁	15.58545	175,455	1	2	0	-1	0	0	-1	0	0	0	0	324	-17	-2.1	0.1
	15.58765	175,465	1	2	0	-1	1	0	-1	0	0	0	1	323	-16	-0.4	0.0
So ₁	16.05697	183,555	1	3	-2	0	0	0	0	0	0	-2	0	194	-8	-0.2	0.0
	16.12989	185,355	1	3	0	-2	0	0	-2	0	0	0	0	185	-7	-0.1	0.0
Oo ₁	16.13911	185,555	1	3	0	0	0	0	0	0	-2	0	-2	184	-7	-0.6	0.0
	16.14131	185,565	1	3	0	0	1	0	0	0	-2	0	-1	184	-7	-0.4	0.0
	16.14352	185,575	1	3	0	0	2	0	0	0	-2	0	0	184	-7	-0.1	0.0
ν_1	16.68348	195,455	1	4	0	-1	0	0	-1	0	-2	0	-2	141	-4	-0.1	0.0
	16.68569	195,465	1	4	0	-1	1	0	-1	0	-2	0	-1	141	-4	-0.1	0.0

The variation of $k_{20}^{(0)}$ across the zonal tidal band, $(nm) = (20)$, is due to mantle anelasticity; it is described by the formula

$$k_{20}^{(0)} = 0.29525 - 5.796 \times 10^{-4} \left\{ \cot \frac{\alpha\pi}{2} \left[1 - \left(\frac{f_m}{f} \right)^\alpha \right] + i \left(\frac{f_m}{f} \right)^\alpha \right\} \quad (6.12)$$

on the basis of the anelasticity model referred to earlier. Here f is the frequency of the zonal tidal constituent, f_m is the reference frequency equivalent to a period of 200 s, and $\alpha = 0.15$. The δk_f in Table 6.5b are the differences between $k_{20}^{(0)}$ computed from the above formula and the nominal value $k_{20} = 0.30190$ given in Table 6.3.

The total variation in geopotential coefficient \bar{C}_{20} is obtained by adding to the result of Step 1 the sum of the contributions from the tidal constituents listed in Table 6.5b computed using Equation (6.8a). The tidal variations in \bar{C}_{2m} and \bar{S}_{2m} for the other m are computed similarly, except that Equation (6.8b) is to be used together with Table 6.5a for $m = 1$ and Table 6.5c for $m = 2$.

Table 6.5b: Corrections for frequency dependence of $k_{20}^{(0)}$ of the zonal tides due to anelasticity. Units: 10^{-12} . The nominal value k_{20} for the zonal tides is taken as 0.30190. The real and imaginary parts δk_f^R and δk_f^I of δk_f are listed, along with the corresponding in-phase (*ip*) amplitude ($A_0 H_f \delta k_f^R$) and out-of-phase (*op*) amplitude ($A_0 H_f \delta k_f^I$) to be used in Equation (6.8a).

Name	Doodson No.	deg/hr	τ	s	h	p	N'	p_s	ℓ	ℓ'	F	D	Ω	δk_f^R	Amp. (<i>ip</i>)	δk_f^I	Amp. (<i>op</i>)
	55,565	0.00221	0	0	0	0	1	0	0	0	0	0	1	0.01347	16.6	-0.00541	-6.7
	55,575	0.00441	0	0	0	0	2	0	0	0	0	0	2	0.01124	-0.1	-0.00488	0.1
S_a	56,554	0.04107	0	0	1	0	0	-1	0	-1	0	0	0	0.00547	-1.2	-0.00349	0.8
S_{sa}	57,555	0.08214	0	0	2	0	0	0	0	0	-2	2	-2	0.00403	-5.5	-0.00315	4.3
	57,565	0.08434	0	0	2	0	1	0	0	0	-2	2	-1	0.00398	0.1	-0.00313	-0.1
	58,554	0.12320	0	0	3	0	0	-1	0	-1	-2	2	-2	0.00326	-0.3	-0.00296	0.2
M_{sm}	63,655	0.47152	0	1	-2	1	0	0	1	0	0	-2	0	0.00101	-0.3	-0.00242	0.7
	65,445	0.54217	0	1	0	-1	-1	0	-1	0	0	0	-1	0.00080	0.1	-0.00237	-0.2
M_m	65,455	0.54438	0	1	0	-1	0	0	-1	0	0	0	0	0.00080	-1.2	-0.00237	3.7
	65,465	0.54658	0	1	0	-1	1	0	-1	0	0	0	1	0.00079	0.1	-0.00237	-0.2
	65,655	0.55366	0	1	0	1	0	0	1	0	-2	0	-2	0.00077	0.1	-0.00236	-0.2
M_{sf}	73,555	1.01590	0	2	-2	0	0	0	0	0	0	-2	0	-0.00009	0.0	-0.00216	0.6
	75,355	1.08875	0	2	0	-2	0	0	-2	0	0	0	0	-0.00018	0.0	-0.00213	0.3
M_f	75,555	1.09804	0	2	0	0	0	0	0	0	-2	0	-2	-0.00019	0.6	-0.00213	6.3
	75,565	1.10024	0	2	0	0	1	0	0	0	-2	0	-1	-0.00019	0.2	-0.00213	2.6
	75,575	1.10245	0	2	0	0	2	0	0	0	-2	0	0	-0.00019	0.0	-0.00213	0.2
M_{stm}	83,655	1.56956	0	3	-2	1	0	0	1	0	-2	-2	-2	-0.00065	0.1	-0.00202	0.2
M_{tm}	85,455	1.64241	0	3	0	-1	0	0	-1	0	-2	0	-2	-0.00071	0.4	-0.00201	1.1
	85,465	1.64462	0	3	0	-1	1	0	-1	0	-2	0	-1	-0.00071	0.2	-0.00201	0.5
M_{sqm}	93,555	2.11394	0	4	-2	0	0	0	0	0	-2	-2	-2	-0.00102	0.1	-0.00193	0.2
M_{qm}	95,355	2.18679	0	4	0	-2	0	0	-2	0	-2	0	-2	-0.00106	0.1	-0.00192	0.1

6.2.2 Treatment of the permanent tide

The degree 2 zonal tide generating potential has a mean (time average) value that is nonzero. This time independent $(nm) = (20)$ potential produces a permanent deformation and a consequent time independent contribution to the geopotential coefficient \bar{C}_{20} . In formulating a geopotential model, two approaches may be taken (see Chapter 1). When the time independent contribution is included in the adopted value of \bar{C}_{20} , then the value is termed “zero tide” and will be noted

Table 6.5c: Amplitudes ($A_2\delta k_f H_f$) of the corrections for frequency dependence of $k_{22}^{(0)}$, taking the nominal value k_{22} for the sectorial tides as $(0.30102 - i0.00130)$. Units: 10^{-12} . The corrections are only to the real part.

Name	Doodson No.	deg/hr	τ	s	h	p	N'	p_s	ℓ	ℓ'	F	D	Ω	δk_f^R	Amp.
N_2	245,655	28.43973	2	-1	0	1	0	0	1	0	2	0	2	0.00006	-0.3
M_2	255,555	28.98410	2	0	0	0	0	0	0	0	2	0	2	0.00004	-1.2

here \bar{C}_{20}^{zt} . If the time independent contribution is not included in the adopted value of \bar{C}_{20} , then the value is termed “conventional tide free” and will be noted here \bar{C}_{20}^{tf} .

In the case of a “zero tide” geopotential model, the model of tidal effects to be added should not once again contain a time independent part. One must not then use the expression (6.6) as it stands for modeling $\Delta\bar{C}_{20}$; its permanent part must first be restored. This is Step 3 of the computation, which provides $\Delta\bar{C}_{20}^{zt}$, to be used with a “zero tide” geopotential model.

$$\Delta\bar{C}_{20}^{zt} = \Delta\bar{C}_{20} - \Delta\bar{C}_{20}^{perm} \quad (6.13)$$

where $\Delta\bar{C}_{20}$ is given by Equation (6.6) and where $\Delta\bar{C}_{20}^{perm}$ is the time-independent part:

$$\Delta\bar{C}_{20}^{perm} = A_0 H_0 k_{20} = (4.4228 \times 10^{-8})(-0.31460)k_{20}. \quad (6.14)$$

In the case of EGM2008, the difference between the zero-tide and tide-free value of C_{20} is -4.1736×10^{-9} . Assuming the same values for A_0 , H_0 and k_{20} , the tide-free value of C_{20} corresponding to Table 6.2 would be $-0.48416531 \times 10^{-3}$.

The use of “zero tide” values and the subsequent removal of the effect of the permanent tide from the tide model is presented for consistency with the 18th IAG General Assembly Resolution 16.

6.3 Effect of the ocean tides

The dynamical effects of ocean tides are most easily incorporated as periodic variations in the normalized Stokes’ coefficients of degree n and order m $\Delta\bar{C}_{nm}$ and $\Delta\bar{S}_{nm}$. These variations can be evaluated as

$$[\Delta\bar{C}_{nm} - i\Delta\bar{S}_{nm}](t) = \sum_f \sum_+ (C_{f,nm}^\pm \mp iS_{f,nm}^\pm) e^{\pm i\theta_f(t)}, \quad (6.15)$$

where $C_{f,nm}^\pm$ and $S_{f,nm}^\pm$ are the geopotential harmonic amplitudes (see more information below) for the tide constituent f , and where $\theta_f(t)$ is the argument of the tide constituent f as defined in the explanatory text below Equation (6.8e).

Ocean tide models are typically developed and distributed as gridded maps of tide height amplitudes. These models provide in-phase and quadrature amplitudes of tide heights for selected, main tidal frequencies (or main tidal waves), on a variable grid spacing over the oceans. Using standard methods of spherical harmonic decomposition and with the use of an Earth loading model, the maps of ocean tide height amplitudes have been converted to spherical harmonic coefficients of the geopotential, and provided for direct use in Equation (6.15). This computation follows Equation (6.21) and has been carried out for the tide model proposed in Section 6.3.2.

Typically, an ocean tide model provides maps for only the largest tides or main waves. The spectrum of tidal geopotential perturbations can be completed by interpolation from the main waves to the smaller, secondary waves, using an assumption of linear variation of tidal admittance between closely spaced tidal frequencies. For each secondary wave, the geopotential harmonic amplitudes can be derived from the amplitudes of two nearby main lines, or pivot waves, (labeled with subscripts 1 and 2) as

$$\begin{aligned} C_{f,nm}^{\pm} &= \frac{\dot{\theta}_f - \dot{\theta}_1}{\dot{\theta}_2 - \dot{\theta}_1} \cdot \frac{H_f}{H_2} C_{2,nm}^{\pm} + \frac{\dot{\theta}_2 - \dot{\theta}_f}{\dot{\theta}_2 - \dot{\theta}_1} \cdot \frac{H_f}{H_1} C_{1,nm}^{\pm} \\ S_{f,nm}^{\pm} &= \frac{\dot{\theta}_f - \dot{\theta}_1}{\dot{\theta}_2 - \dot{\theta}_1} \cdot \frac{H_f}{H_2} S_{2,nm}^{\pm} + \frac{\dot{\theta}_2 - \dot{\theta}_f}{\dot{\theta}_2 - \dot{\theta}_1} \cdot \frac{H_f}{H_1} S_{1,nm}^{\pm} \end{aligned} \quad (6.16)$$

where H is the astronomic amplitude of the considered wave. See an example in Table 6.7 developed for the main waves of FES2004 (see Section 6.3.2).

Some background information on the determination of the coefficients is given in Section 6.3.1, and is included here for completeness. It is not necessary for the evaluation of tidal perturbations to the geopotential. Information on selected tidal models and their use is provided in Section 6.3.2.

6.3.1 Background on ocean tide models

Ocean tide models are conventionally expressed in terms of amplitude and phase of waves at certain discrete frequencies.

$$\xi(\phi, \lambda, t) = \sum_f Z_f(\phi, \lambda) \cos(\theta_f(t) - \psi_f(\phi, \lambda)) \quad (6.17)$$

where Z_f is the amplitude of wave f , ψ_f is the phase at Greenwich and θ_f is the Doodson argument, see the explanatory text below Equation (6.8e).

When expanding amplitudes (Z_f) and phases (ψ_f) of the different waves of tides (from cotidal grids) in spherical harmonic functions of $Z_f \cos(\psi_f)$ and $Z_f \sin(\psi_f)$, it yields:

$$\xi(\phi, \lambda, t) = \sum_f \sum_{n=1}^N \sum_{m=0}^n \bar{P}_{nm}(\sin \phi) \sum_{\pm} \xi_{f,nm}^{\pm}(\lambda, t) \quad (6.18)$$

where

$$\xi_{f,nm}^{\pm}(\lambda, t) = \bar{C}_{f,nm}^{\pm} \cos(\theta_f + \chi_f \pm m\lambda) + \bar{S}_{f,nm}^{\pm} \sin(\theta_f + \chi_f \pm m\lambda) \quad (6.19)$$

The couples of coefficients ($\bar{C}_{f,nm}^{\pm}, \bar{S}_{f,nm}^{\pm}$) represent prograde and retrograde normalized spherical harmonic coefficients of the main wave f at degree n and order m , and can be alternately expressed in terms of amplitude $\hat{C}_{f,nm}^{\pm}$ and phase $\varepsilon_{f,nm}^{\pm}$ such as:

$$\begin{aligned} \bar{C}_{f,nm}^{\pm} &= \hat{C}_{f,nm}^{\pm} \sin(\varepsilon_{f,nm}^{\pm}) \\ \bar{S}_{f,nm}^{\pm} &= \hat{C}_{f,nm}^{\pm} \cos(\varepsilon_{f,nm}^{\pm}) \end{aligned} \quad (6.20)$$

The χ_f values agree with the so-called Shureman convention which is traditionally applied in cotidal maps. They comply with the Doodson-Warburg convention which is defined according to the sign of the harmonic amplitude H_f (see Table 6.6 according to Cartwright and Eden, 1973).

For each wave f , the coefficients $C_{f,nm}^{\pm}$ and $S_{f,nm}^{\pm}$ to be used in Equation (6.15) can be computed as

$$\begin{aligned} C_{f,nm}^{\pm} &= \frac{4\pi G \rho_w}{g_e} \left(\frac{1+k'_n}{2n+1} \right) \hat{C}_{f,nm}^{\pm} \sin(\varepsilon_{f,nm}^{\pm} + \chi_f) \\ S_{f,nm}^{\pm} &= \frac{4\pi G \rho_w}{g_e} \left(\frac{1+k'_n}{2n+1} \right) \hat{C}_{f,nm}^{\pm} \cos(\varepsilon_{f,nm}^{\pm} + \chi_f) \end{aligned} \quad (6.21)$$

Table 6.6: Values of the phase bias χ_f according to the sign of H_f

	$H_f > 0$	$H_f < 0$
$n_1=0$, long period wave	π	0
$n_1=1$, diurnal wave	$\frac{\pi}{2}$	$-\frac{\pi}{2}$
$n_1=2$, semi-diurnal wave	0	π

where G and g_e are given in Chapter 1, ρ_w is the density of seawater (1025 kg m⁻³) and where k'_n is the load deformation coefficient of degree n ($k'_2 = -0.3075$, $k'_3 = -0.195$, $k'_4 = -0.132$, $k'_5 = -0.1032$, $k'_6 = -0.0892$).

6.3.2 Ocean tide models

The practical implementation of ocean tide models in this form begins with identification of the underlying ocean tide height model. Once this model is identified, further needed information can include the specification of maximum degree and order of the expansion, the identification of the pivot waves for interpolation, the special handling (if necessary) of the solar (radiational) tides, or the long-period tidal bands.

For the case of the FES2004 ocean tide model, these details of implementation are provided next.

FES2004

The FES2004 ocean tide model (Lyard *et al.*, 2006) includes long period waves (S_a , S_{sa} , M_m , M_f , M_{tm} , M_{sqm}), diurnal waves (Q_1 , O_1 , P_1 , K_1), semi-diurnal waves ($2N_2$, N_2 , M_2 , T_2 , S_2 , K_2) and the quarter-diurnal wave (M_4 ⁵). For direct use in Equation (6.15), the coefficients $C_{f,nm}^\pm$ and $S_{f,nm}^\pm$ for the main tidal waves of FES2004 can be found at <⁶>

The tide height coefficients can be found in the file <⁷>, both in the form of the coefficients $\bar{C}_{f,nm}^\pm$ and $\bar{S}_{f,nm}^\pm$ and in the form of the amplitudes $\hat{C}_{f,nm}^\pm$ and phases $\varepsilon_{f,nm}^\pm$, as defined in Equations (6.19) and (6.20). They have been computed up to degree and order 100 by quadrature method from quarter-degree cotidal grids. Then ellipsoidal corrections to spherical harmonics were applied (Balmino, 2003) in order to take into account that tidal models are described on the oblate shape of the Earth.

Table 6.7 provides a list of admittance waves which can be taken into account to complement the model. It indicates the pivot waves for linear interpolation following Equation (6.16), where indices 1 and 2 refer to the two pivot waves.

It is to be noticed that radiational waves like S_1 and S_2 require special handling, since the common altimetric models (including FES2004) for these tides include the contributions of atmospheric pressure variations on the ocean height (i.e. the radiational tide). As a result, neither S_1 and S_2 are used as pivot waves for interpolation in Table 6.7. While an S_2 wave is available as a part of the FES2004 model, a mean S_1 wave is given outside FES2004 and available in file <⁸>.

The additionally provided mean S1 wave should only be used in case the gravitational influences of mass transport from an ocean circulation model like MOG2D (Carrère and Lyard, 2003) are not also modeled. This is because the S1 signal is generally part of such ocean circulation models provided with an interval of 6 hours.

Moreover, very long period waves like Ω_1 (18.6 yr) and Ω_2 (9.3 yr) which are not yet correctly observed can be modeled as equilibrium waves. Their amplitudes (and phases) are computed from the astronomical amplitude H_f considering the elastic response of the Earth through the Love numbers:

⁵The χ value for M_4 , not given in Table 6.6, is 0

⁶ftp://tai.bipm.org/iers/conv2010/chapter6/tidemodels/fes2004_Cnm-Snm.dat

⁷<ftp://tai.bipm.org/iers/conv2010/chapter6/tidemodels/fes2004.dat>

⁸<ftp://tai.bipm.org/iers/conv2010/chapter6/tidemodels/S1.dat>

$$\hat{C}_{f,20} = \frac{1 + k_2 - h_2}{\sqrt{4\pi}} |H_f|, \quad \epsilon_{f,20} = -\frac{\pi}{2}$$

where $k_2 = 0.29525$ and $h_2 = 0.6078$ are the Love numbers of potential and deformation, respectively.

Influence of tidal models

For a satellite like Stella (altitude 800 km, inclination 98.7° and eccentricity 0.001), for one day of integration, the effects of ocean tides are typically of order several cm and can reach 20 cm. It is estimated that the main waves of the FES2004 model typically represent 80% of the effect (Biancale, 2008).

For Starlette (altitude 800 km, inclination 49.8° and eccentricity 0.02) and Lageos1 (altitude 5900 km, inclination 109.8° and eccentricity 0.005), integration time of 6 and 7 days, respectively, showed a 3-D RMS difference (mostly along-track) of 9 and 7 mm, respectively, for the difference between FES2004 and the older CSR3.0 ocean tide model (Ries, 2010).

Table 6.7: List of astronomical amplitudes H_f (m) for main waves of FES2004 (in bold) and for some secondary waves (with their pivot waves when they have to be linearly interpolated).

Darwin's symbol	Doodson's number	H_f	Pivot wave 1	Pivot wave 2
Ω_1	055.565	.02793		
Ω_2	055.575	-.00027		
S_a	056.554	-.00492		
S_{sa}	057.555	-.03100		
S_{ta}	058.554	-.00181	057.555	065.455
M_{sm}	063.655	-.00673	057.555	065.455
	065.445	.00231	057.555	065.455
M_m	065.455	-.03518		
	065.465	.00229	065.455	075.555
	065.555	-.00375	065.455	075.555
	065.655	.00188	065.455	075.555
M_{sf}	073.555	-.00583	065.455	075.555
	075.355	-.00288	065.455	075.555
M_f	075.555	-.06663		
	075.565	-.02762	075.555	085.455
	075.575	-.00258	075.555	085.455
M_{stm}	083.655	-.00242	075.555	085.455
	083.665	-.00100	075.555	085.455
M_{tm}	085.455	-.01276		
	085.465	-.00529	085.455	093.555
M_{sqm}	093.555	-.00204		
	095.355	-.00169	085.455	093.555
	117.655	-.00194	135.455	145.555
$2Q_1$	125.755	-.00664	135.655	145.555
σ_1	127.555	-.00802	135.655	145.555
σ_1	135.645	-.00947	135.655	145.555
Q₁	135.655	-.05020		
	137.445	-.00180	135.655	145.555
ρ_1	137.455	-.00954	135.655	145.555
	145.545	-.04946	135.655	145.555
O₁	145.555	-.26221		
	145.755	.00170	145.555	165.555
τ_1	147.555	.00343	145.555	165.555
	153.655	.00194	145.555	165.555
	155.455	.00741	145.555	165.555

continued

Darwin's symbol	Doodson's number	H_f	Pivot wave 1	Pivot wave 2
	155.555	-.00399	145.555	165.555
M_1	155.655	.02062	145.555	165.555
	155.665	.00414	145.555	165.555
χ_1	157.455	.00394	145.555	165.555
π_1	162.556	-.00714	145.555	165.555
P_1	163.555	-.12203		
S_1	164.556	.00289		
K_{1-}	165.545	-.00730	145.555	165.555
K_1	165.555	.36878		
K_{1+}	165.565	.05001	145.555	165.555
ψ_1	166.554	.00293	145.555	165.555
φ_1	167.555	.00525	145.555	165.555
θ_1	173.655	.00395	145.555	165.555
J_1	175.455	.02062	145.555	165.555
	175.465	.00409	145.555	165.555
S_{01}	183.555	.00342	145.555	165.555
	185.355	.00169	145.555	165.555
O_{01}	185.555	.01129	145.555	165.555
	185.565	.00723	145.555	165.555
ν_1	195.455	.00216	145.555	165.555
$3N_2$	225.855	.00180	235.755	245.655
ϵ_2	227.655	.00467	235.755	245.655
$2N_2$	235.755	.01601		
μ_2	237.555	.01932	235.755	245.655
	245.555	-.00389	237.755	245.655
	245.645	-.00451	237.755	245.655
N_2	245.655	.12099		
ν_2	247.455	.02298	245.655	255.555
γ_2	253.755	-.00190	245.655	255.555
α_2	254.556	-.00218	245.655	255.555
	255.545	-.02358	245.655	255.555
M_2	255.555	.63192		
β_2	256.554	.00192	255.555	275.555
λ_2	263.655	-.00466	255.555	275.555
L_2	265.455	-.01786	255.555	275.555
	265.555	.00359	255.555	275.555
	265.655	.00447	255.555	275.555
	265.665	.00197	255.555	275.555
T_2	272.556	.01720	255.555	275.555
S_2	273.555	.29400		
R_2	274.554	-.00246	255.555	275.555
K_2	275.555	.07996		
K_{2+}	275.565	.02383	255.555	275.555
K_{2++}	275.575	.00259	255.555	275.555
η_2	285.455	.00447	255.555	275.555
	285.465	.00195	255.555	275.555
M_4	455.555			

6.4 Solid Earth pole tide

The pole tide is generated by the centrifugal effect of polar motion, characterized by the potential

$$\begin{aligned}
 \Delta V(r, \theta, \lambda) &= -\frac{\Omega^2 r^2}{2} \sin 2\theta (m_1 \cos \lambda + m_2 \sin \lambda) \\
 &= -\frac{\Omega^2 r^2}{2} \sin 2\theta \operatorname{Re} [(m_1 - im_2) e^{i\lambda}].
 \end{aligned}
 \tag{6.22}$$

(See Section 7.1.4 for further details, including the relation of the wobble variables (m_1, m_2) to the polar motion variables (x_p, y_p) .) The deformation which constitutes this tide produces a perturbation

$$-\frac{\Omega^2 r^2}{2} \sin 2\theta \operatorname{Re} [k_2 (m_1 - im_2) e^{i\lambda}]$$

in the external potential, which is equivalent to changes in the geopotential coefficients C_{21} and S_{21} . Using for k_2 the value $0.3077 + 0.0036i$ appropriate to the polar tide yields

$$\begin{aligned} \Delta \bar{C}_{21} &= -1.333 \times 10^{-9} (m_1 + 0.0115m_2), \\ \Delta \bar{S}_{21} &= -1.333 \times 10^{-9} (m_2 - 0.0115m_1), \end{aligned}$$

where m_1 and m_2 are in seconds of arc.

6.5 Ocean pole tide

The ocean pole tide is generated by the centrifugal effect of polar motion on the oceans. This centrifugal effect is defined in Equation (6.22) from Section 6.4. Polar motion is dominated by the 14-month Chandler wobble and annual variations. At these long periods, the ocean pole tide is expected to have an equilibrium response, where the displaced ocean surface is in equilibrium with the forcing equipotential surface.

Desai (2002) presents a self-consistent equilibrium model of the ocean pole tide. This model accounts for continental boundaries, mass conservation over the oceans, self-gravitation, and loading of the ocean floor. Using this model, the ocean pole tide produces the following perturbations to the normalized geopotential coefficients, as a function of the wobble variables (m_1, m_2) .

$$\begin{bmatrix} \Delta \bar{C}_{nm} \\ \Delta \bar{S}_{nm} \end{bmatrix} = R_n \left\{ \begin{bmatrix} \bar{A}_{nm}^R \\ \bar{B}_{nm}^R \end{bmatrix} (m_1 \gamma_2^R + m_2 \gamma_2^I) + \begin{bmatrix} \bar{A}_{nm}^I \\ \bar{B}_{nm}^I \end{bmatrix} (m_2 \gamma_2^R - m_1 \gamma_2^I) \right\} \quad (6.23a)$$

where

$$R_n = \frac{\Omega^2 a_E^4}{GM} \frac{4\pi G \rho_w}{g_e} \left(\frac{1 + k'_n}{2n + 1} \right) \quad (6.23b)$$

and

Ω , a_E , GM , g_e , and G are defined in Chapter 1,

ρ_w = density of sea water = 1025 kgm^{-3} ,

k'_n = load deformation coefficients ($k'_2 = -0.3075$, $k'_3 = -0.195$, $k'_4 = -0.132$, $k'_5 = -0.1032$, $k'_6 = -0.0892$),

$\gamma = \gamma_2^R + i\gamma_2^I = (1 + k_2 - h_2) = 0.6870 + i0.0036$

(Values of k_2 and h_2 appropriate for the pole tide are as given in Sections 6.4 and 7.1.4),

(m_1, m_2) are the wobble parameters in radians. Refer to Section 7.1.4 for the relationship between the wobble variables (m_1, m_2) and the polar motion variable (x_p, y_p) .

The coefficients from the self-consistent equilibrium model, $\bar{A}_{nm} = \bar{A}_{nm}^R + i\bar{A}_{nm}^I$ and $\bar{B}_{nm} = \bar{B}_{nm}^R + i\bar{B}_{nm}^I$, are provided to degree and order 360 at $\langle 9 \rangle$.

The $(n, m) = (2, 1)$ coefficients are the dominant terms of the ocean pole tide. Using the values defined above yields the following $(n, m) = (2, 1)$ coefficients for the ocean pole tide:

$$\begin{aligned} \Delta \bar{C}_{21} &= -2.1778 \times 10^{-10} (m_1 - 0.01724m_2), \\ \Delta \bar{S}_{21} &= -1.7232 \times 10^{-10} (m_2 - 0.03365m_1), \end{aligned} \quad (6.24)$$

⁹ftp://tai.bipm.org/iers/conv2010/chapter6/desaiscopolecoef.txt

where m_1 and m_2 are in seconds of arc. Approximately 90% of the variance of the ocean pole tide potential is provided by the degree $n = 2$ spherical harmonic components, with the next largest contributions provided by the degree $n = 1$ and $n = 3$ components, respectively (see Figure 6.1). Expansion to spherical harmonic degree $n = 10$ provides approximately 99% of the variance. However, adequate representation of the continental boundaries will require a spherical harmonic expansion to high degree and order. The degree $n = 1$ components are shown in Figure 6.1 to illustrate the size of the ocean pole tide contribution to geocenter motion but these terms should not be used in modeling station displacements.

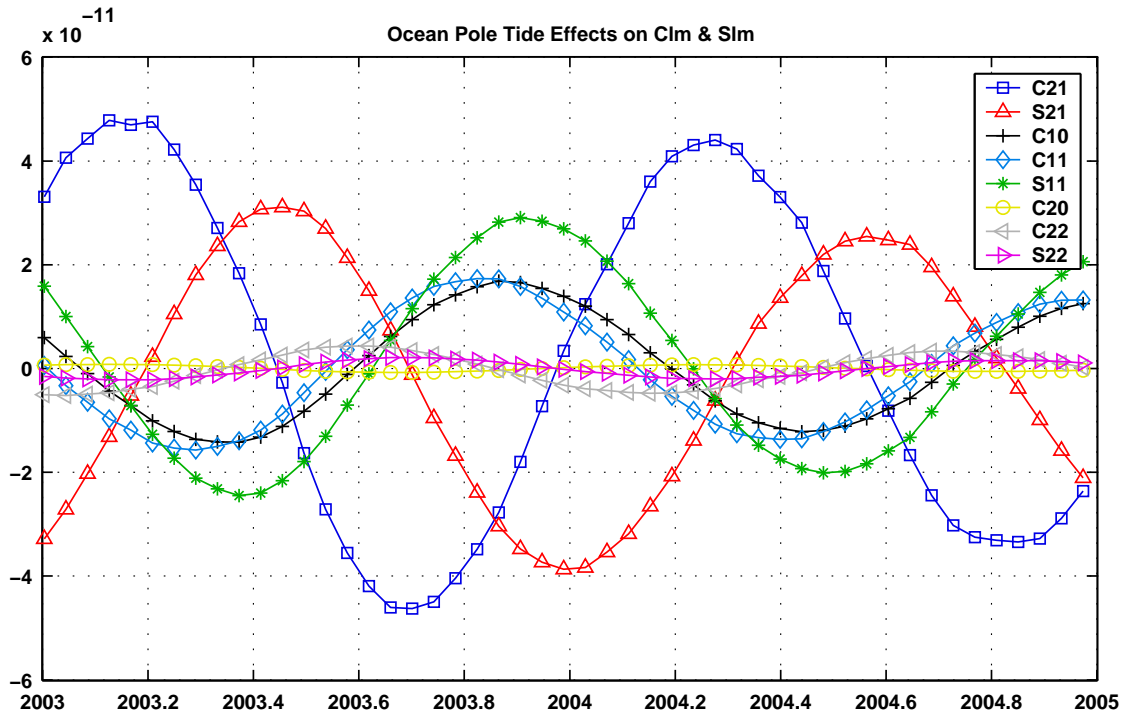


Figure 6.1: Ocean pole tide: first spherical harmonic components.

6.6 Conversion of tidal amplitudes defined according to different conventions

The definition used for the amplitudes of tidal terms in the recent high-accuracy tables differ from each other and from Cartwright and Tayler (1971). Hartmann and Wenzel (1995) tabulate amplitudes in units of the potential (m^2s^{-2}), while the amplitudes of Roosbeek (1996), which follow the Doodson (1921) convention, are dimensionless. To convert them to the equivalent tide heights H_f of the Cartwright-Tayler convention, multiply by the appropriate factors from Table 6.5. The following values are used for the constants appearing in the conversion factors: Doodson constant $D_1 = 2.63358352855 \text{ m}^2 \text{ s}^{-2}$; $g_e \equiv g$ at the equatorial radius = 9.79828685 (from $GM = 3.986004415 \times 10^{14} \text{ m}^3 \text{ s}^{-2}$, $R_e = 6378136.55 \text{ m}$).

Table 6.8: Factors for conversion to Cartwright-Tayler amplitudes from those defined according to Doodson's and Hartmann and Wenzel's conventions.

From Doodson	From Hartmann & Wenzel
$f_{20} = -\frac{\sqrt{4\pi}}{\sqrt{5}} \frac{D_1}{g_e} = -0.426105$	$f'_{20} = \frac{2\sqrt{\pi}}{g_e} = 0.361788$
$f_{21} = -\frac{2\sqrt{24\pi}}{3\sqrt{5}} \frac{D_1}{g_e} = -0.695827$	$f'_{21} = -\frac{\sqrt{8\pi}}{g_e} = -0.511646$
$f_{22} = \frac{\sqrt{96\pi}}{3\sqrt{5}} \frac{D_1}{g_e} = 0.695827$	$f'_{22} = \frac{\sqrt{8\pi}}{g_e} = 0.511646$
$f_{30} = -\frac{\sqrt{20\pi}}{\sqrt{7}} \frac{D_1}{g_e} = -0.805263$	$f'_{30} = \frac{2\sqrt{\pi}}{g_e} = 0.361788$
$f_{31} = \frac{\sqrt{720\pi}}{8\sqrt{7}} \frac{D_1}{g_e} = 0.603947$	$f'_{31} = \frac{\sqrt{8\pi}}{g_e} = 0.511646$
$f_{32} = \frac{\sqrt{1440\pi}}{10\sqrt{7}} \frac{D_1}{g_e} = 0.683288$	$f'_{32} = \frac{\sqrt{8\pi}}{g_e} = 0.511646$
$f_{33} = -\frac{\sqrt{2880\pi}}{15\sqrt{7}} \frac{D_1}{g_e} = -0.644210$	$f'_{33} = -\frac{\sqrt{8\pi}}{g_e} = -0.511646$

References

- Balmino, G., 2003, "Ellipsoidal corrections to spherical harmonics of surface phenomena gravitational effects,," *Special publication in honour of H. Moritz*, Technical University of Graz, pp. 21–30.
- Biancale, R., 2008, personal communication.
- Carrère, L. and Lyard, F., 2003, "Modeling the barotropic response of the global ocean to atmospheric wind and pressure forcing - comparison with observations," *Geophys. Res. Lett.* **30(6)**, 1275, doi: 10.1029/2002GL016473.
- Cartwright, D. E. and Tayler, R. J., 1971, "New computations of the tide-generating potential," *Geophys. J. Roy. astr. Soc.*, **23(1)**, pp. 45–73., doi: 10.1111/j.1365-246X.1971.tb01803.x.
- Cartwright, D. E. and Edden, A. C., 1973, "Corrected tables of tidal harmonics," *Geophys. J. Roy. astr. Soc.*, **33(3)**, pp. 253–264, doi: 10.1111/j.1365-246X.1973.tb03420.x.
- Casotto, S., 1989, "Nominal ocean tide models for TOPEX precise orbit determination," Ph.D. dissertation, The Univ. of Texas at Austin.
- Chapman, S. and Lindzen, R., 1970, *Atmospheric Tides*, D. Reidel, Dordrecht, 200 pp.
- Chao, B. F., Ray, R. D., Gipson, J. M., Egbert, G. D. and Ma, C., 1996, "Diurnal/semidiurnal polar motion excited by oceanic tidal angular momentum," *J. Geophys. Res.*, **101(B9)**, pp. 20151–20163, doi: 10.1029/96JB01649.
- Cheng, M.K., Shum, C.K., Tapley, B.D., 1997, "Determination of long-term changes in the Earth's gravity field from satellite laser ranging observations," *J. Geophys. Res.*, **102(B10)**, pp. 22377–22390, doi:10.1029/97JB01740.
- Cheng, M. K., Ries, J. C., and Tapley, B. D., 2010, "Variations of the Earth's figure axis from satellite laser ranging and GRACE," *J. Geophys. Res.*, submitted.
- Desai, S. D. and Wahr, J. M., 1995, "Empirical ocean tide models estimated from Topex/Poseidon altimetry," *J. Geophys. Res.*, **100(C12)**, pp. 25205–25228.
- Desai, S. D., 2002, "Observing the pole tide with satellite altimetry," *J. Geophys. Res.*, **107(C11)**, 3186, doi:10.1029/2001JC001224.
- Doodson, A. T., 1921, "The Harmonic development of the tide-generating potential," *Proc. R. Soc. A.*, **100**, pp. 305–329.
- Dziewonski, A. and Anderson, D. L., 1981, "Preliminary reference earth model," *Phys. Earth Planet. In.*, **25**, pp. 297–356.
- Eanes, R. J., Schutz, B., and Tapley, B., 1983, "Earth and ocean tide effects on Lageos and Starlette," in *Proc. of the Ninth International Symposium on Earth Tides*, Kuo, J. T. (ed.), E. Schweizerbart'sche Verlagabuchhandlung, Stuttgart.
- Eanes R. J. and Bettadpur, S., 1995, "The CSR 3.0 global ocean tide model," *Technical Memorandum CSR-TM-95-06*, Center for Space Research, University of Texas, Austin, TX.
- Flechtner, F., 2007, "AOD1B Product Description Document," GRACE project document 327-750, Rev. 3.1.
- Hartmann, T. and Wenzel, H.-G., 1995, "The HW95 tidal potential catalogue," *Geophys. Res. Lett.*, **22(24)**, pp. 3553–3556, doi:10.1029/95GL03324.
- Lyard, F., Lefevre, F., Letellier, T., Francis, O., 2006, "Modelling the global ocean tides: modern insights from FES2004," *Ocean Dyn.*, **56(5-6)**, pp. 394–415, doi: 10.1007/s10236-006-0086-x.
- Mathews, P. M., Buffett, B. A., and Shapiro, I. I., 1995, "Love numbers for diurnal tides: Relation to wobble admittances and resonance expansions," *J. Geophys. Res.*, **100(B9)**, pp. 9935–9948, doi:10.1029/95JB00670.

- Mathews, P. M., Herring, T. A., and Buffett, B. A., 2002, "Modeling of nutation-precession: New nutation series for nonrigid Earth, and insights into the Earth's interior," *J. Geophys. Res.*, **107**(B4), doi: 10.1029/2001JB000390.
- Mayer-Gürr, T., "ITG-Grace03s: The latest GRACE gravity field solution computed in Bonn," Joint International GSTM and DFG SPP Symposium Potsdam, 15-17 October 2007, see http://www.igg.uni-bonn.de/apmg/fileadmin/DatenModelle/media/mayer-guerr_gstm_potsdam_2007.pdf.
- Nerem, R. S., Chao, B. F., Au, A. Y., Chan, J. C., Klosko, S. M., Pavlis, N. K. and Williamson, R. G., 1993, "Temporal variations of the Earth's gravitational field from satellite laser ranging to Lageos," *Geophys. Res. Lett.*, **20**(7), pp. 595–598, doi: 10.1029/93GL00169.
- Pavlis, N. K., Holmes, S. A., Kenyon, S. C., and Factor, J. K., 2008, "An Earth gravitational model to degree 2160: EGM2008," presented at the 2008 General Assembly of the European Geosciences Union, Vienna, Austria, April 13-18, 2008, see http://earth-info.nga.mil/GandG/wgs84/gravitymod/egm2008/NPavlis&al_EGU2008.ppt.
- Ray, R. D. and Cartwright, D. E., 1994, "Satellite altimeter observations of the M_f and M_m ocean tides, with simultaneous orbit corrections," *Gravimetry and Space Techniques Applied to Geodynamics and Ocean Dynamics*, Geophysical Monograph 82, IUGG Volume 17, pp. 69–78.
- Ries, J.C., 2010, personal communication.
- Roosbeek, F., 1996, "RATGP95: a harmonic development of the tide-generating potential using an analytical method," *Geophys. J. Int.*, **126**(1), pp. 197–204, doi: 10.1111/j.1365-246X.1996.tb05278.x.
- Schwiderski, E., 1983, "Atlas of ocean tidal charts and maps, Part I: The semi-diurnal principal lunar tide M₂," *Mar. Geod.*, **6**(3-4), pp. 219–265, doi: 10.1080/15210608309379461.
- Souchay, J. and Folgueira, M., 1998, "The effect of zonal tides on the dynamical ellipticity of the Earth and its influence on the nutation," *Earth, Moon and Planets*, **81**(3), pp. 201–216, doi: 10.1023/A:1006331511290.
- Wahr, J. M., 1981, "The forced nutations of an elliptical, rotating, elastic, and oceanless Earth," *Geophys. J. Roy. Astron. Soc.*, **64**(3), pp. 705–727, doi: 10.1111/j.1365-246X.1981.tb02691.x.
- Wahr, J., 1987, "The Earth's C_{21} and S_{21} gravity coefficients and the rotation of the core," *Geophys. J. Roy. astr. Soc.*, **88**, pp. 265–276.
- Wahr, J. M. and Sasao, T., 1981, "A diurnal resonance in the ocean tide and the Earth's load response due to the resonant free "core nutation"," *Geophys. J. Roy. astr. Soc.*, **64**, pp. 747–765.
- Wahr, J., 1990, "Corrections and update to 'The Earth's C_{21} and S_{21} gravity coefficients and the rotation of the core'," *Geophys. J. Int.*, **101**, pp. 709–711.
- Wahr, J. and Bergen, Z., 1986, "The effects of mantle elasticity on nutations, Earth tides, and tidal variations in the rotation rate," *Geophys. J. Roy. astr. Soc.*, **87**, 633–668.
- Widmer, R., Masters, G., and Gilbert, F., 1991, "Spherically symmetric attenuation within the Earth from normal mode data," *Geophys. J. Int.*, **104**, pp. 541–553.